Inorganica Chimica Acta, 128 (1987) 31–37

Mechanism for the Oxidative Addition of Iodomethane to Carbonyl(*N*-hydroxy-*N*-nitrosobenzenaminato-*O*,*O'*)triarylphosphinerhodium(I) Complexes and Crystal Structure of [Rh(cupf)(CO)(CH_3)(I)(PPh_3)]

S. S. BASSON*, J. G. LEIPOLDT, A. ROODT and J. A. VENTER

Department of Chemistry, University of the Orange Free State, Bloemfontein 9300, South Africa

(Received August 18, 1986)

Abstract

Rh(I) complexes, [Rh(cupf)(CO)(PX_3)] (cupf = cupferrate; PX_3 = PCy_3, P(*o*-Tol)$_3$, PPh_3, $PPh_2C_6F_5$, P(*p*-ClC_6H_4)$_3$ and P(*p*-$MeOC_6H_4$)$_3$), react with iodomethane to form Rh(III) alkyl compounds. The reaction was studied in the solvents Bz, EtOAc, Me_2CO, MeOH, CH_3CN and DMSO having different polarities and donocities. The reaction proceeds through two competing rate determining steps, one of which is first-order in [CH_3I]. A reaction mechanism, which includes specific solvent effects, is given. The structure determination of [Rh(cupf)(CO)(CH_3)(I)(PPh_3)] shows the complex to crystallize in space group $P\bar{1}$ with a = 9.912(2), b = 11.534(1), c = 12.514(2) Å, α = 67.84(2), β = 84.41(2), γ = 73.15(1)°, Z = 2 and D_m = 1.73 g cm^{-3}. The molecule has distorted octahedral geometry with CH_3 and I *cis*-bonded. Bond distances: Rh–I = 2.708(2), Rh–P = 2.327(4), Rh–O(hydroxy) = 2.04(1), Rh–O(nitroso) = 2.175(9), Rh–C(carbonyl) = 1.81(2) and Rh–C(methyl) = 2.08(1) Å. Rates for the slow alkyl → acyl conversion in Me_2CO and CH_3CN are also given for this complex.

Introduction

We have recently reported [1, 2] on the oxidative addition of iodomethane to [Rh(LL)(CO)(PX_3)] complexes (LL = β-diketones, X = Ph, *p*-PhCl or *p*-PhOMe) for which the results were strongly in favour of an ionic S_N2 two-step operative mechanism. The latter implies a *trans* geometry of addition for the alkyl halide. A concerted three-center *cis* addition with retention of configuration at the carbon atom of the alkyl halide [3] is a well-known alternative operating for example exclusively in the case of homonuclear molecules like hydrogen [4] and other unsymmetrical substrates like silanes [5]. A clear-cut choice between the above mechanistic types for a specific reaction is often difficult to make [6] but the nett result for a number of variables during a kinetic study can serve as compelling evidence to exercise this choice. For this reason we chose the cupferrate ligand in a variation of the above formulated Rh(I) complexes since one of the starting complexes, [Rh(cupf)(CO)(PPh_3)] [7], and its oxidative addition product, [Rh(cupf)(CO)(CH_3)(I)(PPh_3)], gave suitable crystals for structure analyses. The ground state stereochemistry of these complexes, although not specific for establishing the mechanistic pathway, could aid the interpretation of the kinetic data for reaction (1). The reactivity of Rh(I) complexes in the latter reaction was also studied with regard to phosphine basicity and bulkiness [8] as well as solvent polarity and donicity effects [9].

$$[Rh(cupf)(CO)(PX_3)] + CH_3I \longrightarrow [Rh(cupf)(CO)(CH_3)(I)(PX_3)] \quad (1)$$

Experimental

Cupferron (ammonium salt of *N*-nitrosophenylhydroxylamine) was recrystallized by precipitating with hexane from a 1:1 acetone/methanol solution to yield a white crystalline product. [Rh(cupf)$(CO)_2$] [7, 10] was used to prepare the [Rh(cupf)(CO)(PX_3)] complexes in an acetone medium according to reaction (2). Small amounts of water were added in each case to enhance crystal growth. The yellow to

$$[Rh(cupf)(CO)_2] + PX_3 \longrightarrow [Rh(cupf)(CO)(PX_3)] + CO \quad (2)$$

yellow–brown products were finally washed with hexane giving yields greater than 60%. CO wavenumbers (cm^{-1}), KBr disk, as follows: PCy_3, 1959; P(*o*-Tol)$_3$, 1971; P(*p*-$MeOC_6H_4$)$_3$, 1971; P(*p*-ClC_6H_4)$_3$, 1977; PPh_3, 1982 and $PPh_2C_6F_5$, 1983.

The oxidative addition product, [Rh(cupf)(CO)(CH_3)(I)(PPh_3)] was prepared as follows: to 0.25 g [Rh(cupf)(CO)(PPh_3)], dissolved in 5 cm^3 acetone, was added 0.67 g CH_3I (10X excess) and the solution

*Author to whom correspondence should be addressed.

0020/1693/87/$3.50

TABLE I. Atomic Coordinates ($\times 10^4$) and Averaged Temperature Factors ($\times 10^3$) (e.s.d.s)

Atom	x	y	z	U_{eq}[a]
Rh	2395(1)	1922(1)	3385.2(9)	37(1)
I	1517(1)	3082(1)	4947(1)	78(1)
N(1)	3306(13)	4256(12)	1965(11)	51(8)
N(2)	4344(12)	3427(11)	2697(10)	40(7)
O(1)	−322(12)	1282(12)	3632(11)	70(8)
O(2)	4288(10)	2268(9)	3432(9)	44(6)
O(3)	2244(12)	3822(10)	2042(10)	57(7)
P	3131(4)	1049(3)	1958(3)	31(2)
C(1)	700(15)	1591(15)	3481(14)	48(9)
C(2)	3000(18)	103(15)	4703(13)	52(10)
C(11)	4845(14)	1260(13)	1467(11)	37(8)
C(12)	5099(16)	2025(15)	350(12)	47(9)
C(13)	6448(18)	2188(17)	41(15)	58(11)
C(14)	7527(16)	1533(16)	882(16)	57(11)
C(15)	7303(17)	743(16)	1962(16)	59(11)
C(16)	5938(15)	592(14)	2288(13)	45(9)
C(21)	3204(13)	−635(12)	2376(10)	32(7)
C(22)	4478(18)	−1610(14)	2568(13)	50(9)
C(23)	4430(19)	−2937(17)	3000(16)	64(12)
C(24)	3148(24)	−3242(16)	3197(14)	66(12)
C(25)	1913(20)	−2264(19)	2972(16)	68(12)
C(26)	1915(17)	−943(15)	2551(14)	55(10)
C(31)	1959(15)	1879(13)	695(13)	43(8)
C(32)	807(15)	2924(12)	640(12)	37(8)
C(33)	−62(15)	3539(14)	−340(13)	46(9)
C(34)	229(18)	3095(15)	−1249(14)	54(10)
C(35)	1385(17)	2010(15)	−1155(14)	54(10)
C(36)	2237(17)	1399(16)	−189(13)	54(10)
C(41)	5594(15)	3821(12)	2704(12)	37(8)
C(42)	6090(16)	4493(14)	1674(14)	48(9)
C(43)	7324(18)	4865(16)	1711(17)	61(11)
C(44)	7970(18)	4547(16)	2764(15)	57(11)
C(45)	7405(17)	3853(15)	3779(14)	52(10)
C(46)	6191(15)	3480(14)	3770(13)	45(9)

[a] $U_{eq} = \frac{1}{3} \sum_i \sum_j [U_{ij}(a_i^* a_j^*)(a_i a_j)]$.

covered with a plastic film for 20 min. Further slow evaporation of the orange solution gave yellow–brown needle-like single crystals suitable for a structure analysis.

Apparatus for visible and IR measurements has been mentioned before [2]. Typical complex concentrations were 1.7×10^{-4} M for the visible and 0.02 M for the IR kinetic measurements. [CH_3I] was varied between 0.17 and 1.02 M thus ensuring good pseudo-first-order plots of $\ln(A_t - A_\infty)$ *versus* time. All kinetic data were fitted for the appropriate equation by using a non-linear least-squares program [2]. All complexes gave a broad absorption maximum at *ca.* 385 nm in the 340–450 nm region. All kinetic measurements were done at this maximum with the following exceptions: PCy_3 at 360 and $PPh_2C_6F_5$ at 370 nm respectively.

Structure Analysis

Crystal data: $RhC_{26}H_{23}IN_2O_3P$, molecular weight 672.3, space group $P\bar{1}$, $a = 9.912(2)$, $b = 11.534(1)$, $c = 12.514(2)$ Å, $\alpha = 67.84(2)$, $\beta = 84.41(2)$, $\gamma = 73.15(1)°$, $Z = 2$, $V = 1268.1$ Å^3, $D_m = 1.73$ g cm^{-3}, μ(Mo Kα) = 19.5 cm^{-1}. Mo Kα radiation (graphite monochromator) $\lambda = 0.71073$ Å, $3 \leqslant \theta \leqslant 23°$, crystal dimensions $0.18 \times 0.18 \times 0.06$ mm was used for intensity data collection. Final R and R_w values were 0.058 and 0.060 respectively for 2177 observed reflections [$I > 3\sigma(I)$] of 3492 independent reflections measured on an Enraf-Nonius CAD4F diffractometer. The intensity data were corrected for Lorentz, polarization effects and crystal decay.

The structure was solved by the heavy atom method and anisotropic refinement performed on all non-hydrogen atoms by least-squares methods using the X-ray 72 system of programs. Atomic scattering factors were those referenced previously [7]. Atomic coordinates and thermal parameters are listed in Table 1.

Results and Discussion

Structure of [Rh(cupf)(CO)(CH_3)(I)(PPh_3)]

A perspective view and atom labelling of the molecule are presented in Fig. 1, whilst Table II gives some selected bond distances and angles. The equatorial array formed by O(2), O(3), C(1) and C(2) is planar with no individual atom displaced by more than 0.044 Å and for the rhodium atom, 0.03 Å, from this plane. The Rh–I bond axis is slightly but significantly

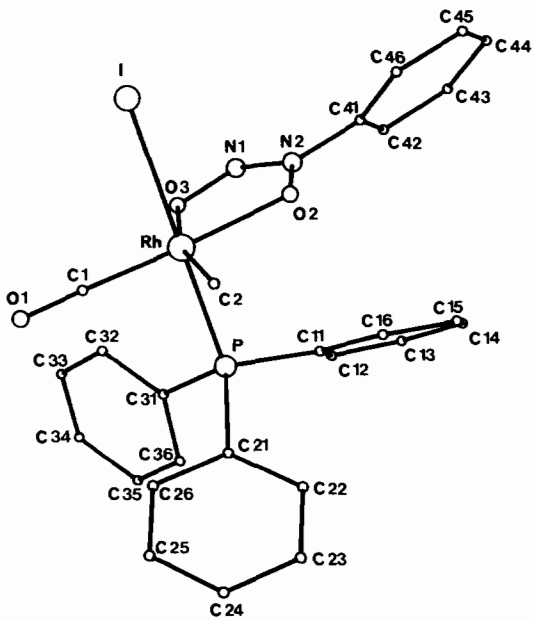

Fig. 1. Perspective view of the [Rh(Cupf)(CO)(CH_3)(I)(PPh_3)] molecule.

TABLE II. Selected Bond Distances and Angles (e.s.d.s)

Distances (Å)			
Rh–O(2)	2.04(1)	P–C(21)	1.79(1)
Rh–O(3)	2.175(9)	P–C(31)	1.83(1)
Rh–C(2)	2.08(1)	O(1)–C(1)	1.14(2)
Rh–C(1)	1.81(2)	O(2)–N(2)	1.32(1)
Rh–I	2.708(2)	O(3)–N(1)	1.27(2)
Rh–P	2.327(4)	N(1)–N(2)	1.33(2)
P–C(11)	1.80(1)	N(2)–C(41)	1.44(2)
Angles (°)			
O(2)–Rh–O(3)	74.9(4)	I–Rh–P	176.6(1)
O(3)–Rh–C(1)	108.1(5)	C(2)–Rh–O(3)	167.3(6)
C(1)–Rh–C(2)	84.6(7)	O(2)–Rh–C(1)	174.8(6)
C(2)–Rh–O(2)	92.4(6)	Rh–C(1)–O(1)	174(1)
O(2)–Rh–P	92.6(3)	Rh–O(3)–N(1)	115.3(8)
O(3)–Rh–P	87.0(4)	Rh–O(2)–N(2)	112.8(7)
C(1)–Rh–P	91.8(6)	O(2)–N(2)–N(1)	124(1)
C(2)–Rh–P	92.5(5)	O(3)–N(1)–N(2)	113(1)
O(2)–Rh–I	86.7(3)	O(2)–N(2)–C(41)	118(1)
O(3)–Rh–I	89.5(4)	N(1)–N(2)–C(41)	118(1)
C(1)–Rh–I	89.1(6)	Rh–P–C(11)	109.2(6)
C(2)–Rh–I	90.8(5)	Rh–P–C(21)	115.2(4)
		Rh–P–C(31)	112.1(5)

inclined by 3.3° towards O(2) and the Rh–P bond, in similar fashion, by 3° towards O(3). These result in a 3.4° deviation from linearity for the I–Rh–P bond axis. The chelate ring atoms are also planar and form an angle of 5.0° with the above-mentioned equatorial plane. The N(2) bonded atoms form an average bond angle of 120(1)°, thus corresponding to a sp^2 hybridized state for this nitrogen atom. The C(41) and C(44) atoms, being displaced by 0.01 and 0.11 Å respectively from the chelate ring-atom plane, can also be considered as part of this plane. Calculations then show that the *N*-substituted phenyl ring is twisted 39.5° along the N(2)–C(41)–C(44) axis relative to the chelate ring-atom plane. This is ascribed to packing considerations if compared with a similar ring-atom-to-equatorial plane angle of 5.2° but a quite different phenyl ring twist of 13.0° in [Rh(cupf)(CO)(PPh_3)] [7].

The most severe deviations from normal octahedral geometry are to be found in the O(2), O(3), C(1), C(2) equatorial plane, especially if the present bond and angle data are compared with those of [Rh(cupf)(CO)(PPh_3)]. The latter complex contains PPh_3 *trans* to O(3) compared with the CH_3 group for the present case, making the two equatorial planes otherwise the same. The Rh–O(3) bond is a significant 0.112 Å longer for the present structure due to the much larger *trans* influence of the CH_3 group. With the Rh–O(2), O(2)–N(2), N(1)–N(2) and O(3)–N(1) distances as well as chelate ring and bite angles being the same within experimental error for the two complexes, it is to be expected that the lengthening of the Rh–O(3) bond, together with different spatial requirements of the PPh_3 and CH_3 groups, will be mainly responsible for any differences between the two equatorial planes. In this respect we notice a formidable increase of 10° for the O(3)–Rh–C(1) and decrease of 9.3° for the O(3)–Rh–C(2) angles in the present structure compared to those of [Rh(cupf)(CO)(PPh_3)]. Similarly, O(2)–Rh–C(2) and C(2)–Rh–C(1) are smaller by 4.4 and 4.1° respectively for the present case. Also, although the O(2)–Rh–C(1) angles of 174.8(6) and 172.8(3)° for the Rh(III) and Rh(I) complexes respectively do not differ very much, inspection of stereo models indicate that the Rh–O(2) and Rh–C(1) bond axes are mainly bent towards O(3) for [Rh(cupf)(CO)(PPh_3)] in contrast to the opposite movement towards C(2) for the present structure. Considering the 5-membered chelate ring as rather rigid, we propose that the lengthening of the Rh–O(3) bond alone cannot be responsible for the clockwise turn of the chelate ring towards C(2), but that the bulkiness of the CH_3 and PPh_3 ligands also play a role. The ligand cone angles [8] of 90 and 145° for CH_3 and PPh_3 respectively could implicate a greater steric demand for the PPh_3 group in the above-mentioned equatorial plane. Complementary to the latter, it was also observed [7] that addition of excess PPh_3 to a solution of [Rh(cupf)(CO)(PPh_3)] did not lead to substitution of the remaining CO group, in line with similar observations on [Rh(β-dik)(CO)(PPh_3)] (β-dik = β-diketones) complexes, but gave instead a trigonal-bipyramidal complex having the two PPh_3 groups *trans*-orientated in the apical positions. However, using $P(OPh)_3$ with a cone angle of 128°, complexes of the type [Rh(β-dik)($P(OPh)_3$)$_2$] could be prepared [11]. The reason for this phenomenon is not clear but both steric and electronic factors should operate since the σ-donor ability of $P(OPh)_3$ is one of the poorest for P(III) derivatives but this is being compensated for in its good π-acid behaviour [12].

Taking a van der Waals radius of 2.0 Å for CH_3 [13] and 1.6 Å for carbon in covalent cyanides [14] and CO further being isoelectronic with CN^-, we consider C(1)····C(2) = 2.63(2) Å as indicative of a strong repulsive interaction between the CO and CH_3 groups. Similar neighbouring contacts of C(2)····P = 3.19(2), C(2)····O(2) = 2.97(2) and I····C(2) = 3.44(2) Å are also repulsive in character. The Rh–C(2) bond distance compares well with other Rh(III) alkyl bonds [15] and with CH_3 as a strong σ-donor, all the above data point to a tight fit of the CH_3 group between neighbouring ligand atoms. The smaller stereochemical demand of CH_3 compared to PPh_3 seems to be the main responsible factor for the observed differences in the aforementioned equatorial planes of the Rh(III) and Rh(I) complexes.

The Rh–I distance of 2.708(2) Å, being slightly longer than the range of 2.60–2.69 Å reported for

complexes having a ligand with a small *trans* influence opposite the Rh–I bond, is however still shorter than the 2.813(1) Å in Rh(I)(CH_3)[C_2(DO)($DOBF_2$)] with CH_3 *trans* to the iodine atom [15, 16]. The present distance thus complies with the concept of PPh_3 having a smaller *trans* influence than an alkyl group. The Rh–P bond is significantly 0.06 Å shorter than the corresponding ones in [Rh(acac)$(I)_2(PPh_3)_2$] [16] containing the *trans*-orientated P–Rh–P moiety, the latter elongation being the result of a mutual *trans* influence. The remaining bond distances in the present structure are considered as normal and need no further comment.

Kinetic Results and Mechanism

The Rh(I) complexes reported here are unstable in solutions of 1,2-dichloroethane, chloroform, tetrahydrofuran and dimethylformamide. Distillation and drying of the solvents, together with exclusion of air (N_2 blanket), did not improve solution stability. In the case of DCE, IR time scans of [Rh(cupf)(CO)-(PPh_3)] indicated the formation of a Rh(III)–CO peak at 2052 cm^{-1}, whilst monitoring at 362 nm in the visible region, gave an oxidative addition rate of $4.8(4) \times 10^{-5}$ s^{-1} at 25 °C in absence of daylight. Normal room illumination gave a more complex reaction indicative of two consecutive rate determining processes. The solvents employed in this study did not show any of the above effects.

All kinetic runs performed in the visible region gave a slow absorbance increase with time corresponding to the rate data reported here. At longer reaction times, the absorbance slowly decreased again indicating further reaction of the oxidative addition product. IR monitoring showed a similar smooth decrease in the Rh(I)–CO peaks and corresponding simultaneous increase of the Rh(III)–CO peaks (2052–2060 cm^{-1}) thus confirming that the first slow process of the visible region is indeed the formation of the oxidative addition product, [Rh(cupf)-(CO)(CH_3)(I)(PX_3)]. To confirm the outcome of the second slow reaction, as well as to investigate any reversible trend in the first Rh(I)–Rh(III) conversion, the stability of [Rh(cupf)(CO)(CH_3)(I)(PPh_3)] was investigated by IR in the absence and presence of CH_3I in acetone and acetonitrile solutions respectively. Time scans indicated in all cases a decrease in the Rh(III)–CO peak and a simultaneous formation of an acyl peak at 1720 cm^{-1}. The second slow process is thus an alkyl → acyl conversion with rates (25 °C) as follows: visible region: acetone, neat, $1.4(1) \times 10^{-3}$ s^{-1}; 1.02 M CH_3I, $1.0(1) \times 10^{-3}$ s^{-1}; acetonitrile, neat, $7.8(5) \times 10^{-4}$ s^{-1}; 1.02 M CH_3I, $1.36(1) \times 10^{-3}$ s^{-1}, IR (2052 cm^{-1}): acetone, neat, $1.3(2) \times 10^{-3}$ s^{-1}; 1.02 M CH_3I, $1.7(5) \times 10^{-3}$ s^{-1}; acetonitrile, neat, $6.5(4) \times 10^{-4}$ s^{-1}; 1.02 M CH_3I, $1.2(6) \times 10^{-3}$ s^{-1}. These IR and corresponding visible data for a specific solvent are the same within experimental error as was also found in control experiments for the oxidative addition step. The above solvent-assisted CO insertions agree with the general mechanistic concepts of this type of reaction [17].

Plots of the pseudo-first-order rate constants, k_{obs}, for the oxidative addition reactions against [CH_3I] gave linear relationships with non-zero intercepts (except in MeOH medium being zero within experimental error) conforming to eqn. (3) where the constants are interpreted in terms of the reaction

$$k_{obs} = k_2 + k_1[CH_3I] \quad (3)$$

scheme. The k_1 and k_2 values, determined in this way, are listed in Tables III and IV for the respective solvent and phosphine variations.

Comparison of the rate constants in Table III with the dielectric constants and solvent donocities shows that, in general, the more polar and/or better donor solvent molecule accelerates the reaction. This can be taken as evidence that the function of the solvent is to ease the charge separation during the rearrangement and formation of the 5-coordinate intermediate (k_1 path) as is also evident from the large negative entropy of activation for acetone medium. In order to make a more realistic comparison between k_1 and k_2 values, we have divided the latter by the respective solvent concentrations (mol dm^{-3}) to obtain the second order rate constants, k_2'. The ratio k_1/k_2' is thus a measure of competition between the CH_3I and

TABLE III. Solvent Effects for the Oxidative Addition of CH_3I to [Rh(cupf)(CO)(PPh_3)] at 25.0 °C (e.s.d.s)

Solvent	ϵ[a]	D_n[a]	10^3k_1 (M^{-1} s^{-1})	10^4k_2 (s^{-1})	$10^5k_2'$ (M^{-1} s^{-1})	k_1/k_2'
Benzene	2.3	0.1	0.0093(5)	0.006(3)	0.0053	175
Ethyl acetate	6.0	17.1	0.229(5)	0.14(3)	0.14	164
Acetone[b]	20.7	17.0	1.22(2)	3.1(1)	2.3	53
Methanol	32.6	19.0	2.5(2)	0.2(1)	–	–
Acetonitrile	38.0	14.1	4.2(2)	7(1)	3.7	114
Dimethylsulfoxide	45.0	29.8	7.8(2)	28(1)	20	39

[a]Ref. 18. [b]$\Delta S_1^* = -180(20)$ and $\Delta S_2^* = -210(30)$ JK^{-1} mol^{-1}; $\Delta H_1^* = 36(5)$ and $\Delta H_2^* = 29(9)$ kJ mol^{-1}, determined from data at four temperatures.

TABLE IV. Rate Constants for Oxidative Addition of CH_3I to [Rh(cupf)(CO)(PX_3)] Complexes in Acetone at 25.0 °C (e.s.d.s)

PX_3	Cone angle (°)[a]	$10^3 k_1$ (M^{-1} s^{-1})	$10^4 k_2$ (s^{-1})
$P(p\text{-}ClC_6H_4)_3$	145	0.193(8)	1.4(5)
PPh_3	145	1.22(2)	3.1(1)
$P(p\text{-}MeOC_6H_4)_3$	145	4.20(8)	2.0(5)
$PPh_2C_6F_5$	158	0.091(9)	0.69(4)
PCy_3	170	1.94(3)	2.4(2)
$P(o\text{-}Tol)_3$	194	0.21(2)	1.9(2)

[a]Ref. 8.

solvent dependent pathways. In the case of DMSO, which is known as a solvent having a good coordinating ability [19], the k_2 path becomes more pronounced relative to k_1 if compared with for example benzene. In a similar sense it can be reasoned that the smaller ratio for acetone compared to acetonitrile reflects the trend in donor numbers but ethyl acetate, on the other hand, having near the same donocity gives a much greater ratio. The style of involvement for the solvent molecule, especially for the k_2 path, is thus not a clear-cut one. In this context it may be noted that the proposed rate determining k_2 path is exactly the same as that for the solvent dependent path of square-planar substitution reactions. Methanol, the only protic solvent in Table III, makes an unexpectedly negligible contribution from the k_2 path to the overall rate. It is the only solvent in the range capable of hydrogen bond formation and being only a σ-donor, differs from ethyl acetate, acetone, acetonitrile and dimethyl sulfoxide containing multiple bonded functional groups. More specific π-bonding stabilization of the transition state for the latter group of biphilic solvents, similarly proposed for S_N2 displacement reactions of Pt(II) complexes [20], are thus expected. Methanol, on the other hand, is a weaker solvating agent [21] but hydrogen-bonding is expected to occur in a transition state (different from those of the biphilic solvents) which will strongly favour the direct attack (k_1 path) of the nucleophilic Rh(I) centre on the polar CH_3I molecule. The greater range (4.7×10^3) for the k_2 rate constants, compared to those of k_1 (0.84×10^3), is also suggestive, apart from polarity effects, of metal–solvent interactions of more specific nature as was also observed in the case of CO insertion reactions [22, 23].

The first three phosphine entries in Table IV have the same stereochemical demand but should influence the Lewis basicity of the Rh(I) centre differently due to the electronegativity differences [24] of the substituent groups. In accordance, the k_1 path shows a 21-fold increase from $P(p\text{-}ClC_6H_4)_3$ to $P(p\text{-}MeOC_6H_4)_3$ which is the expected trend for a nucleophilic attack at the (sp^3)C of iodomethane. To the contrary, the k_2 constants are all, except for $PPh_2C_6F_5$, the same within experimental error. This is also the expected result considering the solvent effects discussed above. If electronic effects [8] alone had been operative for the k_1 path, we would have expected a rate trend of $PCy_3 > P(o\text{-}Tol)_3 \gg PPh_2C_6F_5$ with the three *p*-substituted derivatives interspersed between the latter two. According to Table IV, $k_1(PCy_3) > k_1(P(o\text{-}Tol)_3)$ (in agreement with the electronic effect) but both values are smaller than those of the *p*-methoxy derivative which indicates that a steric influence is also operative. Similarly the $\nu(CO) = 1959$ cm^{-1} for [Rh(cupf)(CO)(PCy_3)] is the lowest for these complexes indicating the good σ-donocity of PCy_3 resulting in the strongest potential Lewis base complex for oxidative addition. For $P(o\text{-}Tol)_3$, comparable to $P(p\text{-}MeOC_6H_4)_3$ in σ-donocity and having the same $\nu(CO)$ values in their respective Rh(I) complexes, we unexpectedly found $\nu(CO) = 2032$ cm^{-1} (compared to the 2050–2060 cm^{-1} range) for the oxidative addition product in acetone medium. This shows that the CO group, due to excessive bulkiness of the phosphine, is possibly shifted to a position implicating strong π-interaction with rhodium. The k_1 rate constant for $PPh_2C_6F_5$ is of the correct expected order indicating a small steric influence if any, but the smaller k_2 value is indicative of an electronic effect if compared with the more bulky phosphines' constants. In this respect we are tempted to ascribe this phenomenon to a neighbouring group participation effect since an *ortho*-substituted electronegative fluorine atom on the phosphine can interact with the metal d_{z^2} orbital similar to the *o*-methoxy interaction in *trans*-[Ir(Cl)(CO){$PMe_2(o\text{-}MeOC_6H_4)$}$_2$] [25]. In such a case the decrease in electron density on the metal could place a restriction on the π-bonded transition state stabilization of the solvent path.

A possible reaction mechanism consistent with the experimental results is shown in Scheme 1. This also includes the ground-state stereochemistries of [Rh(cupf)(CO)(PPh_3)] and the *cis*-addition product, [Rh(cupf)(CO)(CH_3)(I)(PPh_3)]. The k_1 path implies a nucleophilic attack on CH_3I giving the 16-electron 5-coordinate intermediate for which the degree of ion separation will be solvent-dependent. Although these

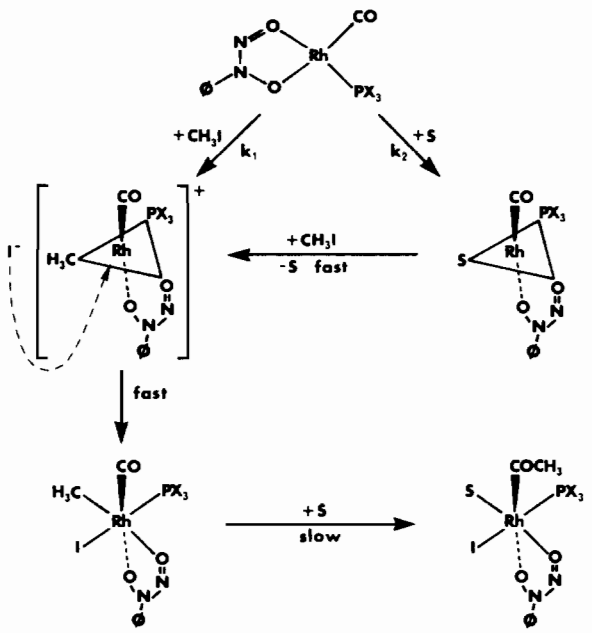

Scheme 1.

trigonal-bipyramidal intermediates can give fast isomerizations, we believe that the constitution of the trigonal plane in the present case is related to the ground-state bond weakening effect of the phosphine ligand in [Rh(cupf)(CO)(PX_3)]. During the Rh–CH_3 bond formation, the CH_3 ligand will tend, based on similar assumptions for square-planar substitution reactions [26], to move towards the least strongly bound ligand (assumed to be the nitroso oxygen) and away from the most strongly bound ligand (assumed to be PX_3), *i.e.*, the folding leading to the formation of the trigonal plane takes place along the diagonal O–Rh–P axis of the Rh(I) complex. Once the Rh–C bond is firmly established, the phosphorous atom can facilitate the simultaneous C–I bond-breaking by π-bond stabilization of the activated complex [27, 28]. The same effect will also facilitate the fast nucleophilic attack of I^- between the Rh–C and Rh–O bonds of the tbp intermediate thus leading, after minor rearrangement, to the *cis* addition product.

The existence of a solvent-stabilized tbp intermediate for the k_2 path is, we believe, justified in terms of the propensity of [Rh(cupf)(CO)(PPh_3)] to add on an extra nucleophilic π-bonding ligand (PPh_3) as well as the reactivity of these complexes towards solvents alone. Secondly, the solvent-assisted k_2 path can be viewed as an oxidative addition catalysis phenomenon similar to the solvent effects in the migratory insertion of CO into transition-metal alkyl bonds (reaction (4)). Most recent research indicates

$$L_nM(CO)R + L' \xrightarrow{S} L_nL'MC(=O)R \qquad (4)$$

that the formation of the 5-coordinate intermediate acyl rather than its coordinative saturation and trapping is the key to the solvent's or nucleophile's role in these insertions [23]. Similarly we could visualize a fast dissociative trapping of the solvent-stabilized tbp intermediate by CH_3I during its conversion to the ionic intermediate of the k_1 path. This solvent-stabilized intermediate, being still a Rh(I) complex, is also expected to be much more reactive towards CH_3I, since the stereochemical transformation, similar to that of the ionic intermediate, has already been taken care of during the k_2 step.

The results of the solvent effects in this study show that it is the major factor responsible for enhancement of oxidation addition rates and we believe also the first example of a solvent-catalyzed pathway. Apart from having a mutual ionic intermediate for the k_1 and k_2 pathways, as depicted in the reaction scheme, this solvent path could also possibly lead to oxidation addition products having for example different stereochemistries. In this respect we notice the mentioning of an additional product (which was not pursued further) for the CH_3I addition to *trans*-[Ir(Cl)(CO){PMe_2(*p*-$MeOC_6H_4$)}$_2$] [25] where an experimental rate law, similar to the present study, was operative. We did not find any evidence for an additional complex during the preparation of [Rh(cupf)(CO)(CH_3)(I)(PPh_3)] but small amounts of a second isomer could go undetected in this way.

Acknowledgements

We wish to thank the South African C.S.I.R. for financial assistance as well as Dr P. H. van Rooyen of the National Chemical Research Laboratory for the intensity data collection.

References

1 S. S. Basson, J. G. Leipoldt and J. T. Nel, *Inorg. Chim. Acta, 84,* 167 (1984).
2 S. S. Basson, J. G. Leipoldt, A. Roodt, J. A. Venter and T. J. van der Walt, *Inorg. Chim. Acta, 119,* 35 (1986).
3 R. G. Pearson and W. R. Muir, *J. Am. Chem. Soc., 92,* 5519 (1970).
4 C. E. Johnson and R. Eisenberg, *J. Am. Chem. Soc., 107,* 3148 (1985).
5 C. E. Johnson and R. Eisenberg, *J. Am. Chem. Soc., 107,* 6531 (1985).
6 R. J. Cross, *Chem. Soc. Rev., 14,* 197 (1985).
7 S. S. Basson, J. G. Leipoldt, A. Roodt and J. A. Venter, *Inorg. Chim. Acta, 118,* L45 (1986).
8 C. A. Tolman, *Chem. Rev., 77,* 313 (1977).
9 V. Gutmann, *Angew. Chem., Int. Ed. Engl., 9,* 843 (1970).
10 K. Goswami and M. M. Singh, *Transition Met. Chem., 5,* 83 (1980).

11 G. J. van Zyl, G. J. Lamprecht and J. G. Leipoldt, *Inorg. Chim. Acta, 102,* L1 (1985).
12 J. Emsley and D. Hall, 'The Chemistry of Phosphorous', Harper and Row, London, 1976.
13 F. A. Cotton and G. Wilkinson, 'Basic Inorganic Chemistry'. Wiley, New York, 1976.
14 D. Britton, in J. D. Dunitz and J. A. Ibers (eds.), 'Perspectives in Structural Chemistry', Vol. 1, Wiley, New York, 1967.
15 J. P. Collman, P. A. Christian, S. Current, P. Denisevich, T. R. Halbert, E. C. Schmittou and K. O. Hodgson, *Inorg. Chem., 15,* 223 (1976).
16 S. S. Basson, J. G. Leipoldt, I. M. Potgieter, A. Roodt and T. J. van der Walt, *Inorg. Chim. Acta, 119,* L9 (1986).
17 A Wojcicki, *Adv. Organomet. Chem., 11,* 87 (1973).
18 U. Mayer and V. Gutmann, *Adv. Inorg. Chem. Radiochem., 17,* 189 (1975).
19 V. I. Baranovskii, Y. N. Kukushkin, N. S. Panina and A. I. Panin, *Russ. J. Inorg. Chem., 18,* 844 (1973).
20 R. G. Pearson, H. B. Gray and F. Basolo, *J. Am. Chem. Soc., 82,* 787 (1960).
21 U. Belluco, U. Croatto, P. Uguagliati and R. Pietropaolo, *Inorg. Chem., 6,* 718 (1967).
22 R. J. Mawby, F. Basolo and R. G. Pearson, *J. Am. Chem. Soc., 86,* 3994 (1964).
23 S. L. Webb, C. M. Giandomenico and J. Halpern, *J. Am. Chem. Soc., 108,* 345 (1986).
24 J. E. Huheey, 'Inorganic Chemistry', 2nd edn., Harper and Row, New York, 1978.
25 E. M. Miller and B. L. Shaw, *J. Chem. Soc., Dalton Trans.,* 480 (1974).
26 K. F. Purcell and J. C. Kotz, 'Inorganic Chemistry', Saunders, Philadelphia, 1977.
27 J. Chatt, L. A. Duncanson and L. M. Venanzi, *J. Chem. Soc.,* 4456 (1955).
28 L. E. Orgel, *J. Inorg. Nucl. Chem., 2,* 137 (1956).